

As submitted to J. Alloys and Compounds, Oct 1997  
Shortened version was published in **268** (1998) 89.

# Formation of $\beta$ -PdD Containing High Deuterium Concentration Using Electrolysis of Heavy-Water

**Edmund Storms**  
2140 Paseo Ponderosa  
Santa Fe, NM 87501

## ABSTRACT

The limiting composition of  $\beta$ -PdD obtained during electrolytic loading results from a complex competition between diffusion of D atoms through any surface barrier, diffusion within the bulk sample, and loss of deuterium gas from surface-penetrating cracks. Reductions in surface-crack concentration and surface-barriers are essential steps to achieve high compositions. The highest compositions within any sample are located within the surface region as a complex patch-work of values. The open circuit voltage (OCV), referenced to platinum, is useful in understanding changes in the surface composition and structure. Values as high as -1.35 V have been observed for highly loaded  $\beta$ -PdD. Evidence for several new, possibly impurity stabilized structures is given.

Key words: (Beta-palladium-deuteride, structure, open-circuit-voltage, loading-efficiency, crack-formation)

## INTRODUCTION

Several properties of beta palladium hydride[1] are enhanced when a high concentration of hydrogen is achieved. However, H/Pd ratios near 1.0 are very difficult to produce for reasons that are not well understood, especially in the Pd-D system.. The electrolytic approach used in this study extends the work of Riley et al.[2] and De Ninno et al. [3] who explored the same problem but used a different approach. A general review of the Pd-H(D) system has been published recently by Flanagan and Oates[4] and should be consulted for important background information.

This work examines the behavior of deuterium once it has entered the palladium lattice and has achieved a high concentration. In contrast, conventional electrolytic studies [5; 6; 7; 8; 9] have explored mechanisms involved in reaction and absorption at the surface using, in most cases,  $\beta$ -PdH. None of the models based on such work adequately describe the behavior of the hydride when very high concentrations of hydrogen are present. These models view the limiting composition to result from a recombination rate at the surface equal to the rate at which atoms are made available by the current, with essentially no transport within the interior. This paper will present evidence for a different model based on almost complete hydrogen transport through the surface, diffusion within the bulk material, and eventual loss through a crack structure.

A crack structure is produced within metals when they react with hydrogen. This structure is caused by increased brittleness and by physical expansion as the hydride is formed. Considerable effort has been devoted to a study of this process [10; 11; 12] in many metals. In contrast, most studies of palladium ignore the phenomenon because the metal shows little visible change and electrochemical studies done at low hydrogen contents are not affected by this problem. However, for the last sixty years [13], hydrogen induced stress in palladium has been known to be relieved by formation of cracks and slip planes when the  $\beta$ -phase is formed, thereby causing marked changes in many properties. For example, a recent paper by De Marco et al.[14] shows how stress produced during hydride formation effects the diffusion rate. Repeated hydriding of

the same piece of palladium produces a gradual change in its physical morphology so that most properties are changed by an additional amount.[15; 16] This behavior is basic to the difficulty in achieving reproducible results when bulk palladium is studied.

Although a variety of defects are produced by hydriding, only those whose presence allows hydrogen gas to migrate through the structure are considered here. When these channels penetrate the surface[17], they provide an avenue for loss of hydrogen when electrolytic loading is used and a portal for entry during gas loading. This paper will concentrate on the consequences of electrolytic loading. On the other hand, completely contained interior cracks can result in blisters[18] and isolated regions of high-pressure gas as electrolysis increases the chemical activity of dissolved hydrogen.[12] Both types of cracks can influence the apparent diffusion rate of hydrogen through the metal, especially at high hydrogen concentrations.

Additional insight into the behavior of cracks is obtained from a study by Storms and Talcott [15] using tritium as a tracer for hydrogen. This work shows that hydrogen, which enters hydrogen-saturated  $\beta$ -PdH during electrolysis, leaves as  $H_2$  gas with a residence time that depends on applied current. In addition, the loss rate is roughly proportional to the crack volume. The authors conclude that most dissolved hydrogen migrates to the surface of cracks where it forms  $H_2$  gas out of contact with the electrolyte. This gas then makes its way through the crack structure to the surface and appears as bubbles at the mouth of cracks. The process does not involve exchange of  $H^+$  ( $D^+$ ) ions at the electrolyte-metal interface as most published models require. Of course, some of these ions absorbed at the surface might recombine to form  $H_2$  ( $D_2$ ) gas before dissolution can take place. This process has been studied extensively[16] and will not be addressed in this paper.

To properly understand the proposed model, the composition at the surface needs to be measured along with the normally measured average composition. A method sensitive to the surface composition is the open-circuit-voltage (OCV). This voltage is measured between the cathode and a stable reference electrode when no current is flowing to or from the cell. The OCV is proportional to the log of the chemical activity of hydrogen (D) at the cathode surface. Of course, this activity will be influenced by impurities[19; 20; 21; 22; 23] deposited on the surface and by changes in crystal structure.[24] Therefore, the relationship between OCV and hydrogen concentration can be very complex. Nevertheless, the OCV is useful in revealing changes in activity, composition, and structure at the surface, as demonstrated in this work and by others [16]. Tanzella et al.[25], Numata and Ohno [26], and Terazawa et al.[27] have used a similar approach to study the loading behavior.

The relationships between deuterium uptake efficiency during electrolysis, maximum composition, open circuit voltage, and deloading behavior were studied. Variations in pretreatment and the loading procedure were explored to discover how deuterium concentrations in the bulk and surface regions might be increased.

## EXPERIMENTAL

### *Material Characteristics*

Ninety samples of palladium sheet (1 cm x 2 cm x 0.1 cm), provided by IMRA Materials (Japan), and a few plates obtained from Johnson Matthey Metals were subjected to various treatments after being polished using 0.5  $\mu$ m diamond slurry. Nominal sample area is 4.1  $cm^2$  when fully loaded and the nominal weight is 2.4 g. The unannealed material contained long, fibrous grains along the rolling direction while the annealed material contained compact grains of various sizes. The annealed samples also showed various degrees of surface reaction, oxygen being the dominant element present. Material annealed in "vacuum" also had silicon on the surface probably as a palladium-silicon-oxygen alloy. Some samples were cleaned using Aqua Regia before delivery and during this work. One-half of the samples contained 500 ppm boron while the rest had less than 1 ppm. Silver is the highest detected impurity at 52 ppm. Radiographic examination shows density variations but no large voids.

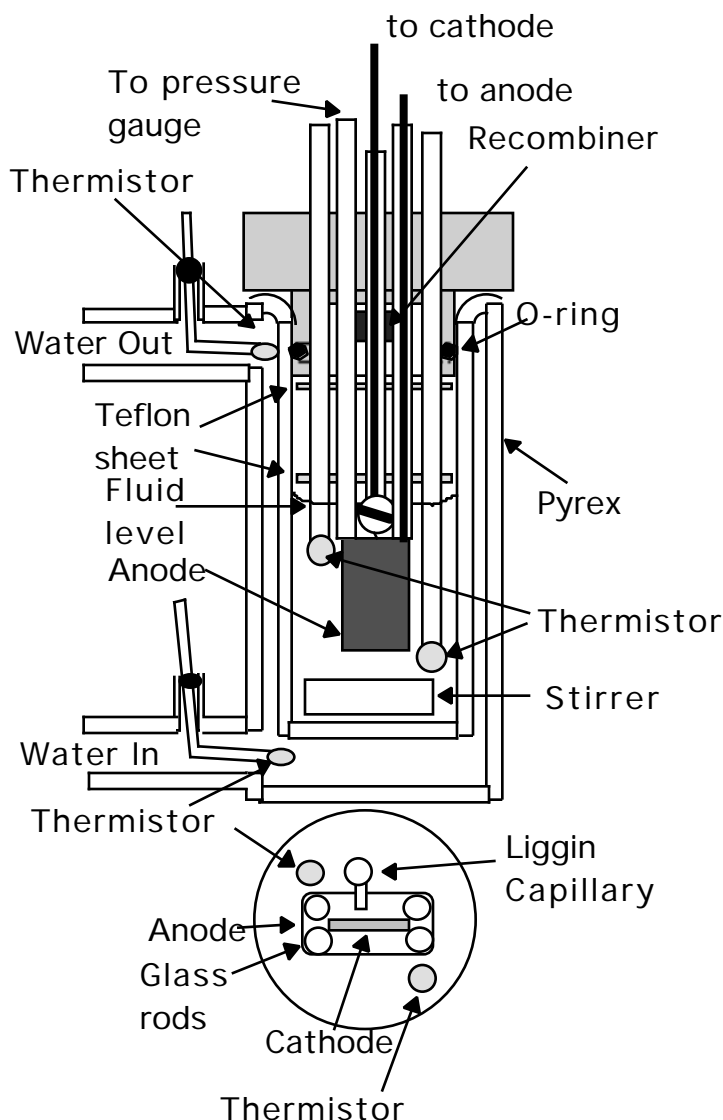


**FIGURE 1.** Cross-section of loading cell

utes, depending on applied current, using the Labview [28] data acquisition program.

A small tube allows oxygen, which remains after deuterium dissolves in the palladium, to displace oil from an external reservoir. This oil is weighed ( $\pm 0.01\text{g}$ ) and used to calculate the D/Pd ratio of the cathode. Although a universal oil constant of  $7300\text{ g oil/mol D}$  can be calculated, a value for each experiment is determined from the increase in cathode weight. The weight ( $\pm 0.00002\text{g}$ ) is measured at known times after the cathode is removed from the cell and the values are extrapolated to zero time. By applying the resulting oil constant to each data point, a relative change in composition is obtained. Unfortunately, the absolute composition is much more uncertain than the relative values because of edge-effects as described below.

Loading efficiency is determined as follows. The applied current,  $I$ , is converted to the amount hydrogen generated during the time interval,  $t$ , using the equation,

A short platinum wire is attached to each sample by drilling a hole and crimping the wire therein. Temperature rise during drilling is avoided by clamping the sample between two pieces of brass. No significant copper is transferred to the palladium by this contact. Preliminary studies show that copper or gold on the cathode structure can dissolve in the electrolyte and plate onto subsequent cathodes. Therefore, the presence of these elements, as well as nickel, was avoided.

The electrolyte is  $0.3\text{ M LiOD}$  with a nominal D/H ratio greater than  $0.995$ , according to the supplier. This solution is made by adding cleaned lithium metal to  $\text{D}_2\text{O}$  in dry air and was stored in a sealed plastic container.

#### *Loading and Measurement of Deuterium Concentration*

Loading is done in a Pyrex cell as shown in Fig. 1. The cell is sealed and contains a catalyst (Pt on graphite) to recombine excess  $\text{D}_2$  and  $\text{O}_2$ . A platinum mesh anode surrounds the cathode within a distance of approximately  $4\text{ mm}$  on all sides. The cell is stirred at a fixed rate ( $300\text{ RPM}$ ) and temperature ( $\pm 0.01^\circ$ ) is measured at two levels. Constant temperature water flows through a surrounding jacket. The apparatus is under computer control and data are taken every 2 to 10 min-

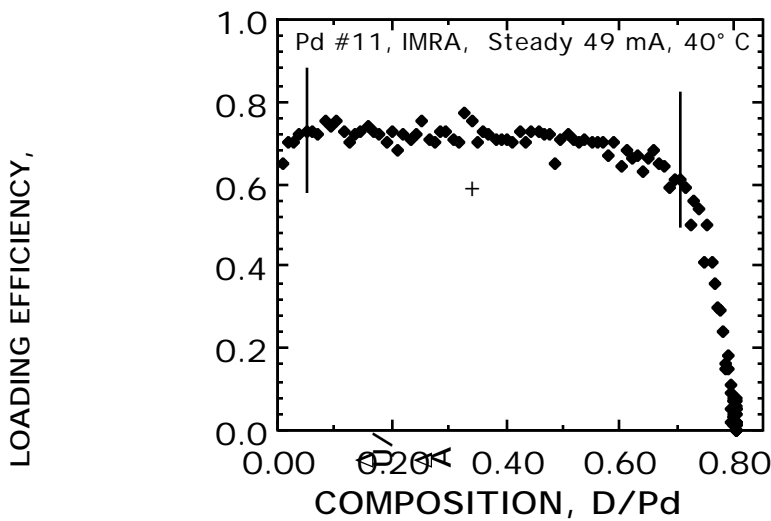


**FIGURE 2.** An example of a high loading efficiency. The composition and  $U/A$  values are not corrected for edge effects. Such corrections move the loading efficiency to near 1.0.

$$A = (\text{Applied Hydrogen}) = I \cdot t / 96496.$$

The amount of hydrogen that reacts with the sample during the same time is calculated using the equation,

$$U = (\text{Used Hydrogen}) = \frac{\text{wt. oil}}{\text{oil/mol D}}.$$

Values obtained using adjacent points taken every 2-10 min are plotted as  $U/A$  vs  $D/Pd$ . When  $U/A$  equals 1.0, all applied deuterium is reacting with the metal. When  $U/A$  equals 0.0, all applied deuterium is leaving the sample as  $D_2$  gas. Typical behavior of "good" palladium is shown in Figure 2.

#### Temperature

The first decision to be made before a sample can be successfully loaded is a choice of temperature. Experience has shown that higher limiting compositions can be achieved when the temperature is low. However, lower temperatures result in steeper concentration and stress gradients. Therefore, the use of higher temperatures during initial loading should reduce the tendency to form cracks. This idea is explored as part of this study. Of course, use of the less convenient gas loading method above the miscibility gap between  $\alpha$ -PdD and  $\beta$ -PdD can completely eliminate this problem.[29] Higher temperatures also provide a higher concentration of glass-dissolution products for deposition on the surface of the cathode. The effect of these impurities may be beneficial. [30]

#### Open Circuit Voltage

Two Luggin capillaries are located within the cell, one on each side of the cathode. One examines a relatively smaller spot and the other measures an average voltage produced by the other side. A flame-cleaned platinum mesh is used as the reference electrode. Although this material does not provide an absolute value for the OCV, it is convenient, it gives a stable potential, and it

introduces no impurities into the cell. Stability is checked by replacing the cathode by clean platinum and noting whether the voltage is equal to zero. A voltage of  $0.00 \pm 0.02$  V is observed between clean palladium and the reference electrode before current is applied. Initial voltages significantly different from zero can be attributed to the presence of impurities on the palladium surface. Values are obtained during loading by interrupting the current to the cell for 5-10 sec. Figure 3 shows a typical relationship between OCV and the average composition (uncorrected

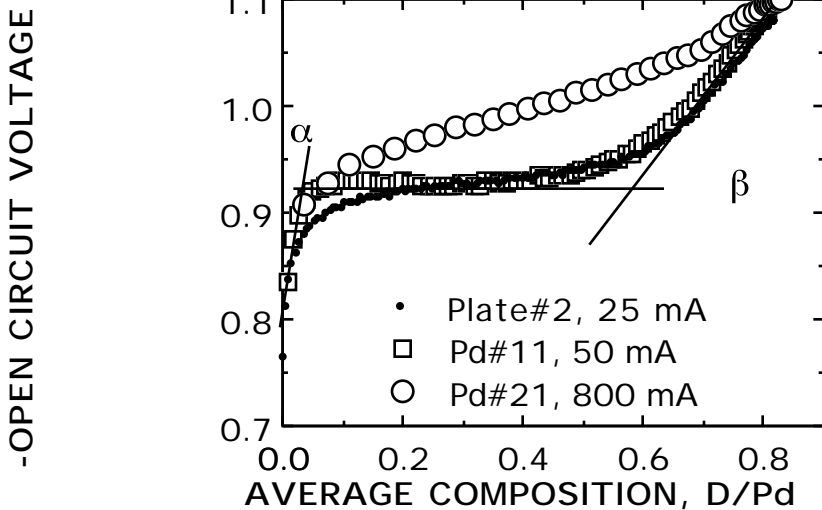


**FIGURE 3.** Typical relationship between OCV and average composition while loading at  $40^\circ\text{C}$  using various currents.

introduces no impurities into the cell. Stability is checked by replacing the cathode by clean platinum and noting whether the voltage is equal to zero. A voltage of  $0.00 \pm 0.02$  V is observed between clean palladium and the reference electrode before current is applied. Initial voltages significantly different from zero can be attributed to the presence of impurities on the palladium surface. Values are obtained during loading by interrupting the current to the cell for 5-10 sec. Figure 3 shows a typical relationship between OCV and the average composition (uncorrected

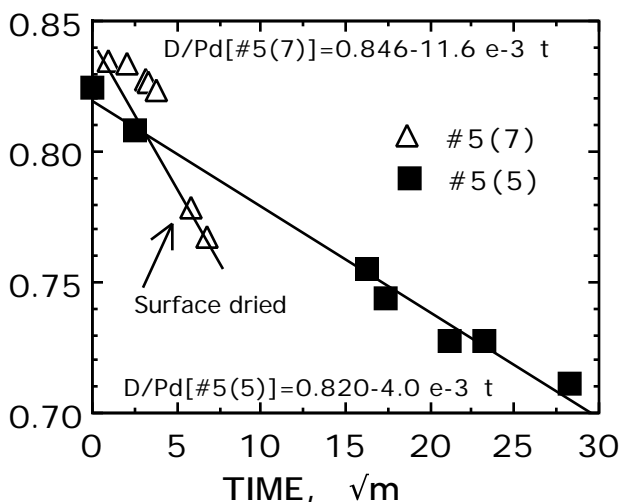


**FIGURE 4.** Deloading at room temperature based on weight change for typical samples. The composition is not corrected for edge effects.

calculate the composition immediately before cell current was interrupted. A typical behavior is shown in Fig. 4 as #5(5). A slope change to a smaller value occurs when the average composition drops below about  $D/Pd=0.6$  [31] because formation of  $\text{-PdD}$  on the surface reduces the diffusion rate. Consequently, quantitative removal of deuterium can be a very slow process that, in some cases, requires use of higher temperatures. A temperature of  $170^\circ\text{C}$  in air is frequently used in this work when complete removal of deuterium is required.

Sample #5(7) shows an example of an initial loss rate that appears to be very small and is nonlinear. This behavior appears to be caused by formation of  $\text{D}_2\text{O}$  on the surface. The vast majority of samples lost  $\text{D}_2$  without visible conversion to  $\text{D}_2\text{O}$  and produced a linear deloading relationship.

#### Data Adjustments

Gas loss from an area about 0.5 mm wide around the edge causes the metal in this region to contain less deuterium compared to the rest of the sample. This deficit is clearly visible because the region expands much less than does the interior, producing a pillow shape. Consequently, the measured average composition, based on the total weight of Pd and D, is lower than the composition within the fully-expanded region. Unfortunately, the magnitude of this effect is dependent on the average composition with a larger effect at high compositions. In addition, the effect is not uniform within a sample or between samples. Therefore, the reported uncorrected D/Pd values are lower limits for the composition that would have resulted had the loading been uniform. The upper limit estimated to be 0.1 larger. This effect would appear to account for many reported differences in achievable composition between plates and wires because the latter exhibit this effect to a much smaller degree. It can also account for some apparent variation between samples.

Edge loss also causes the calculated amount of applied hydrogen, based on applied current, to be too large. In other words, applied current that contacts this deloading edge is wasted as far as loading of the bulk sample is concerned. Electrolytic action at the lead wire also adds a small contribution to this problem. Consequently, values for  $U/A$  must be increased to reflect typical conditions. An average  $U/A$  value of 0.8, measured in this study, is estimated to represent a loading efficiency of 100% for the interior region of the sample. Although these effects make the values less useful as absolute quantities, the relative trends give important insights into mechanisms affecting the loading process.

for edge-effects) for three different currents. The reference electrode is positive with respect to the cathode.

#### Deloading Measurement

Deloading occurs by the loss of  $\text{D}_2$  gas and the rate gives an important insight into the ability of a sample to achieve a high deuterium content. Upon removal from the cell, the samples are weighed at room temperature ( $21\pm 1^\circ\text{C}$ ) at various times starting after about 1 min. Deloading over an extended time shows that deuterium loss from most samples is linear when plotted as a function of square-root of time, a behavior that is consistent with the process being limited by diffusion within the palladium. The slope of the line (DL) was used to compare deloading rates and to

**RESULTS**

*Loading Behavior*

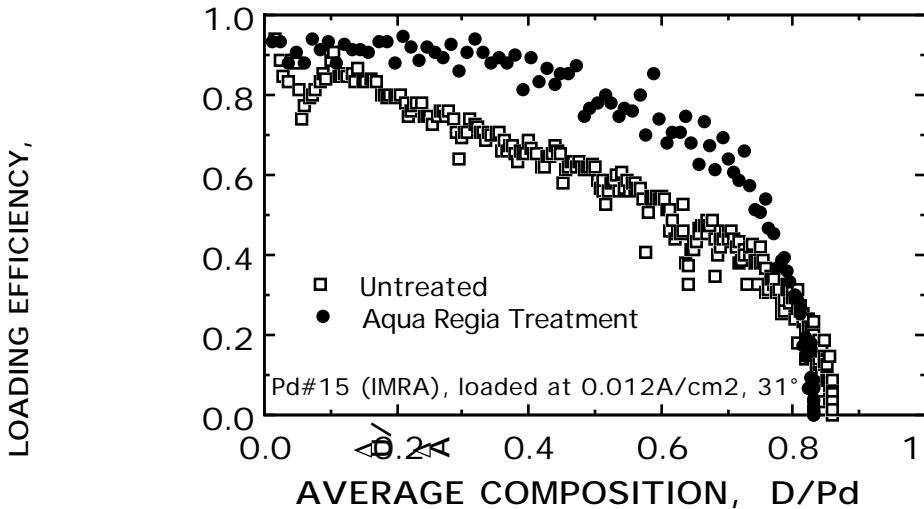


**FIGURE 5.** Effect of Aqua Regia treatment on the loading efficiency. Composition and efficiency are corrected for edge effects.

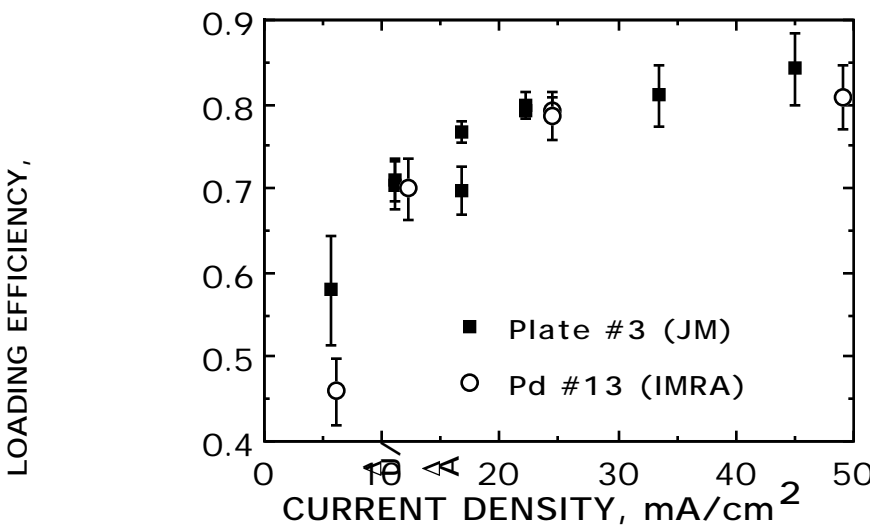


**FIGURE 6.** Loading efficiency of a Pd plate and Pd#13 (after first loading) at 20°C for compositions within the  $\beta$ -phase region.

Some samples of palladium absorb nearly all hydrogen presented to the surface until the average composition exceeds about  $D/Pd=0.6$ . This behavior is also associated with the absence of bubbles at the cathode. A slight initial rise in loading efficiency is often seen as the  $\beta$ -phase becomes saturated and the two-phase region is entered. A nearly constant loading rate frequently occurs when the bulk sample is within the two-phase region. However, this behavior becomes less "ideal" at low temperatures, when high currents are applied, and when a barrier is present on the surface. As the composition increases within the  $\beta$ -phase, the apparent absorption rate

drops to zero when the maximum composition is reached, as can be seen in Figs. 2 and 5. Many samples show evidence for an absorption barrier that reduces the loading rate at all compositions, especially when low currents are used. This barrier can be reduced or removed by using Aqua Regia, as shown in Fig. 5. Variations in this behavior between what appear to be identical samples demonstrate, once again, that many uncontrolled variables are operating, thereby requiring the need to base conclusions on the behavior of more than one sample.

The loading efficiency is also sensitive to applied current. This variable is explored in Fig. 6 for compositions within the two-phase region. Because the values are slightly sensitive to composition, the

plotted values are taken in random sequence in order to reduce the effect of this variable. The efficiency becomes increasingly smaller as the applied current is reduced and approaches an upper limit as current is increased. This is in contrast to the experience of Searson[32] who found the opposite effect. However, the surface of the thin samples used in his study was rapidly converted to the  $\beta$ -phase when high currents were used. Complete conversion will reduce the

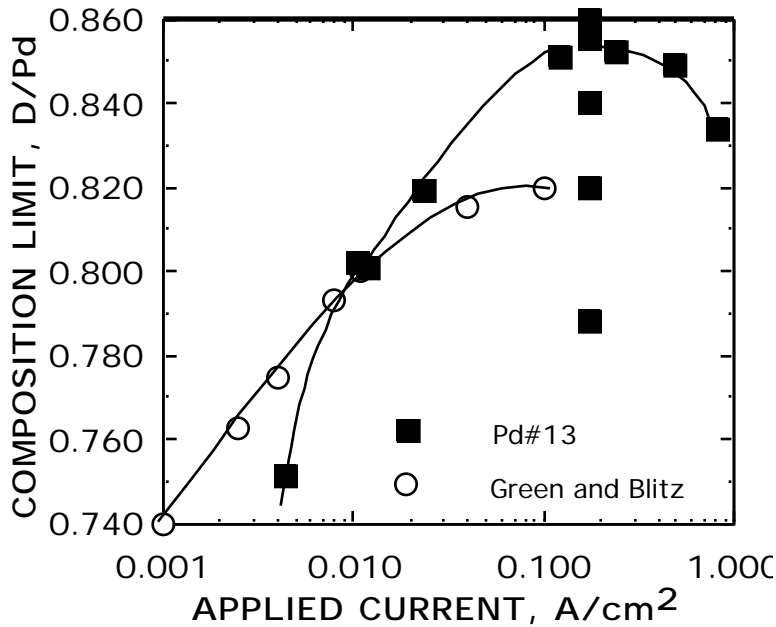


**FIGURE 7.** Limiting, average composition of Pd#13 as a function of applied current density. Curve is drawn through samples at 20° C.

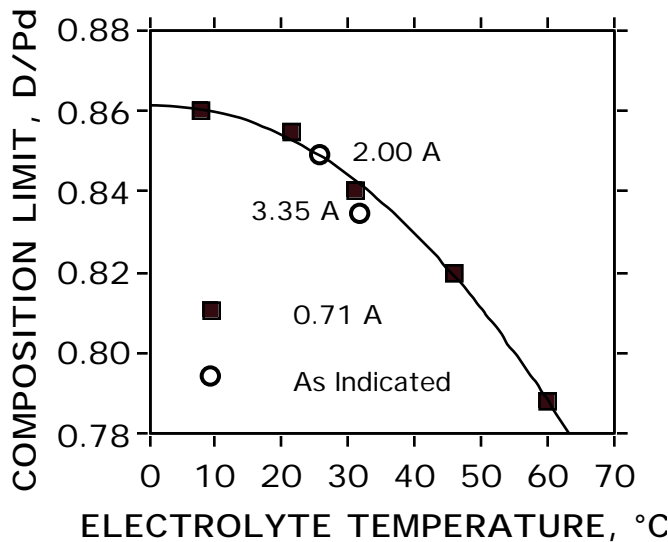


**FIGURE 8.** Effect of temperature on average composition at 0.71 A for Pd#13. Several other indicated currents are compared. The composition is uncorrected for edge-effect.

position is increased. This relationship is unaffected by the temperature or current used to achieve the average composition. In addition, these samples appear to follow the behavior expected based on the internal pressure generated by the average composition. The calculated equilibrium pressure is plotted over the closed points to make this connection clearer. A gradient

apparent loading efficiency and may account for the discrepancy.

The upper composition limit is highly variable between samples. However, regardless of the value achieved after the loading efficiency drops toward zero, a slow improvement will result if current application is continued. In addition, a larger deuterium concentration can be produced by applying a larger current. Figure 7 shows the relationship between applied current density and the limiting composition after steady-state has been achieved. The observed maximum results because sample temperature increases as current is increased. The shape of the relationship below the temperature-induced maximum is similar to

values calculated from the overpotential when 1 M LiOD was used, as reported by Green and Britz[33]

The effect of temperature can be seen in Fig. 8 where the limiting composition is shown as a function of temperature for a current of 0.71 A. Good agreement between the resulting curve and several higher currents indicate that the reduced composition at high currents is caused by increased temperature rather than by increased current.

#### Process of Deloading

The initial deloading rate of all samples falls into one of two sets as shown by the open and closed symbols plotted in Fig. 9. Most samples follow the behavior shown by the closed points, i.e. they have a steeply increasing rate as the average composition

effect is produced a high loss rates because diffusion reduces the composition at the crack surface, hence the loss rate is reduced. Occasionally, a sample is found that behaves like the open points. Such samples are able to achieve very high compositions without the expected high loss rate. The difference between these two patterns of behavior allow palladium to be easily sorted into samples having a useful ability to achieve a very high composition without having to invest excessive time to actually achieve an ultimate

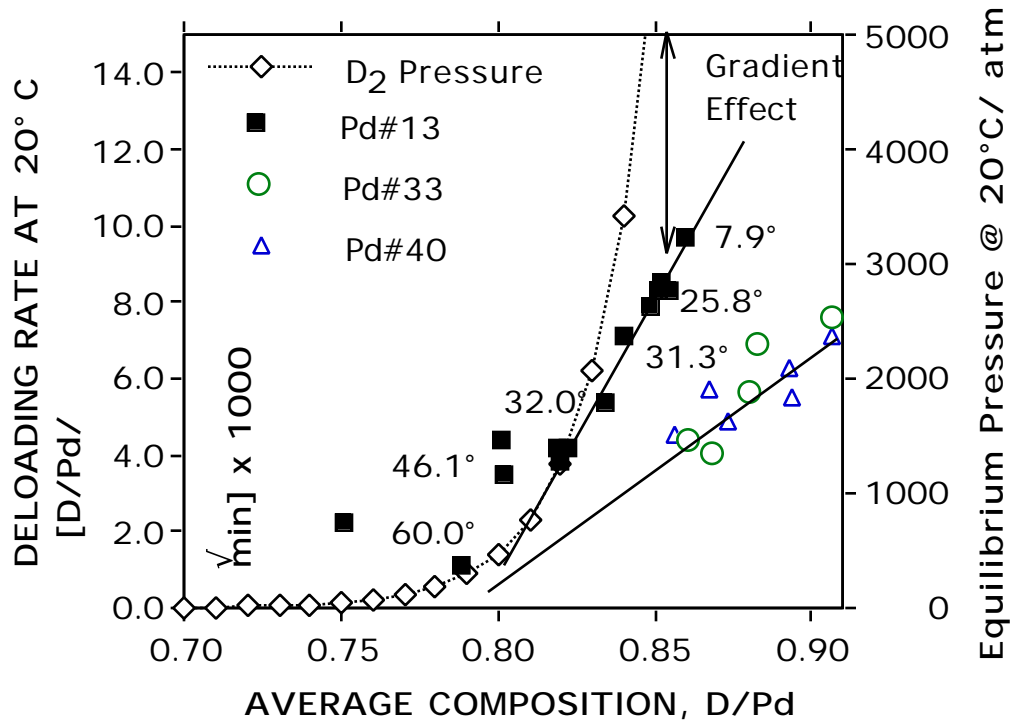


**FIGURE 9.** Deloading rate in air at room temperature as a function of average composition for Pd#13. Composition is not corrected for edge-effect. Equilibrium pressure of D<sub>2</sub> at 20° is shown.

limit. Surface impurities such as Pt, Au or Al also can have unexpected effects on the deloading rate. This complex factor will be the subject of a future paper.

Loss of deuterium is linear with respect to the square root of time even though this relationship is sometimes not apparent when only a few data points are taken. This relationship is clearly shown in Figure 10 for Plate #2 which is deloaded at 40° C in the electrolyte. The initial constant value is caused by a slight inertia in the oil system and initial cooling of the cell after current is interrupted. A break in slope is seen at a composition somewhat higher than where the  $\beta$ -phase would be expected to form on the surface. The deloading rate above the transition is  $5.5 \times 10^{-3}$  D/Pd/ min, a value close to that found when similar samples are deloaded in air. The slope below the composition is reduced because diffusion through the  $\beta$ -phase is slower than through the  $\alpha$ -phase.

The extrapolated atom loss rate immediately after the current is interrupted is nearly equal to the rate at which atoms are being supplied to the sample by the applied current, as shown in Fig.11. For this relationship to occur for all samples, the observed deloading rate would have to be determined only by the loading current. A collection of 40 samples gave average deloading rates of  $8.5 \pm 5.2$  D/Pd/ min for an applied current of 100 mA and  $15.2 \pm 5.8$  D/Pd/ min for 800 mA. Although the trend is in the right direction, the large range of values indicate that other processes are operating including different surface permeabilities and temperatures. Nevertheless, this behavior and previous arguments justify believing that a steady-state, dynamic process occurs after a stable composition has been reached.

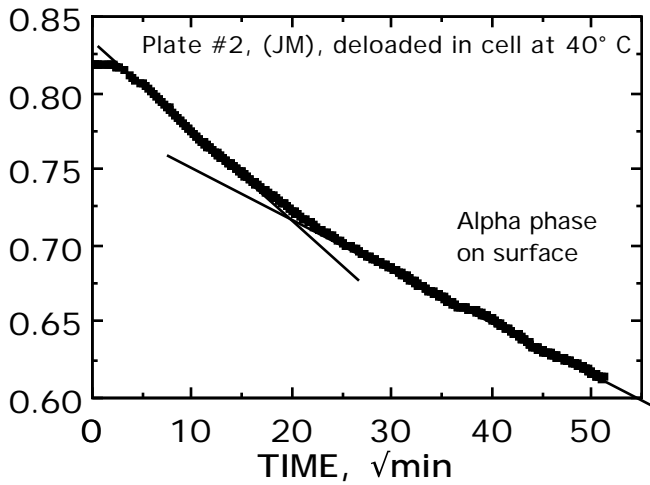


**FIGURE 10.** Plate #2 allowed to deload in the electrolyte while at 40° C. Composition is uncorrected for edge-effect.

ferences that are typically seen between different samples. Changes in slope occur very near compositions expected from the equilibrium phase diagram. In other words, the average composition gives results consistent with a system having a uniform, homogeneous composition between the surface and the interior. This behavior indicates that any composition gradient formed during loading at low current is small and stable until nearly all of the sample has been converted to the  $\beta$ -phase and gas loss through the cracks becomes possible. In addition, the behavior indicates that edge-effects do not cause significant errors in average composition below D/Pd 0.7. However, not all samples have this “ideal” behavior even after being subjected to what appears to be identical treatment and loading conditions. As expected, larger currents

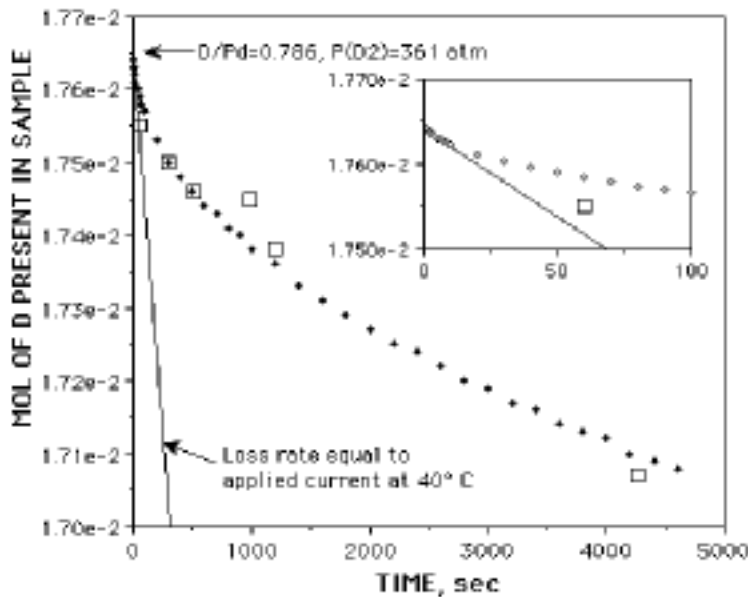


**FIGURE 11.** Pd#5(17) deloading in air at 22° C following an applied current of 200 mA

Most weights were within 0.00005 g of the initial weight after all deuterium is removed from the samples. Therefore, no significant coating is applied during loading. However, some of the boron containing samples are found to have lost about 0.00015 g.

*Open Circuit Voltage*

Several patterns are usually seen in the relationship between OCV and composition. These are a slight rise as  $\beta$ -PdD is loaded, a constant value within the two-phase region, and an increasing value as deuterium is added to the  $\beta$ -phase. This “ideal” behavior can be seen in Fig. 3 for Pd#11. An unannealed palladium plate loaded at a lower current shows a similar behavior but with minor dif-

ferences that are typically seen between different samples. Changes in slope occur very near compositions expected from the equilibrium phase diagram. In other words, the average composition gives results consistent with a system having a uniform, homogeneous composition between the surface and the interior. This behavior indicates that any composition gradient formed during loading at low current is small and stable until nearly all of the sample has been converted to the  $\beta$ -phase and gas loss through the cracks becomes possible. In addition, the behavior indicates that edge-effects do not cause significant errors in average composition below D/Pd 0.7. However, not all samples have this “ideal” behavior even after being subjected to what appears to be identical treatment and loading conditions. As expected, larger currents increase the gradient between the surface and the interior as can be seen in Fig. 3 by the behavior of Pd #21. This shift from ‘equilibrium’ conditions when high currents are applied is typical of all samples although the shape of the resulting curve may differ. Stirring also slightly reduces the absolute values of OCV although relative changes appear to be unaffected.

When samples are allowed to deload within the cell, the OCV has two distinctly different behaviors with variations within each group. Fig. 12 shows deloading of a sample containing a high concentration of deuterium immediately after anomalous heat production had been observed. Such variations in OCV suggest the presence of

-OPEN CIRCUIT VOLTAGE

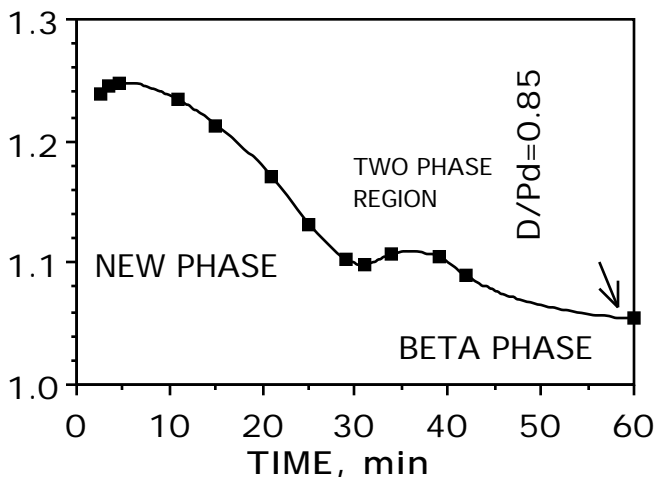


**FIGURE 12.** Open circuit voltage of Pd#42 determined as the sample deloaded within the loading cell at 9.2° C. The uncorrected composition was D/Pd=0.85 at 60 minutes.

(Pd#56) that had a lower OCV showed a different behavior. In general, the higher the OCV, the more complex the behavior. In addition, marked differences in voltage are occasionally found between the two OCV probes, indicating different behaviors between the two sides of the cathode. Samples which were allowed to deload completely generally returned to a zero OCV, showing that surface impurities did not affect the OCV in the absence of deuterium.

The cell-voltage, in contrast to the OCV, does not show a consistent behavior, especially in the  $\beta$ -phase region. As expected, the cell-voltage has been seen to increase at constant current during loading along with an increase in OCV. However, some samples show a decrease in cell-voltage while the OCV increases. Such contrary behavior adds to the difficulty in interpreting reported cell-voltage changes.

-OPEN CIRCUIT VOLTAGE

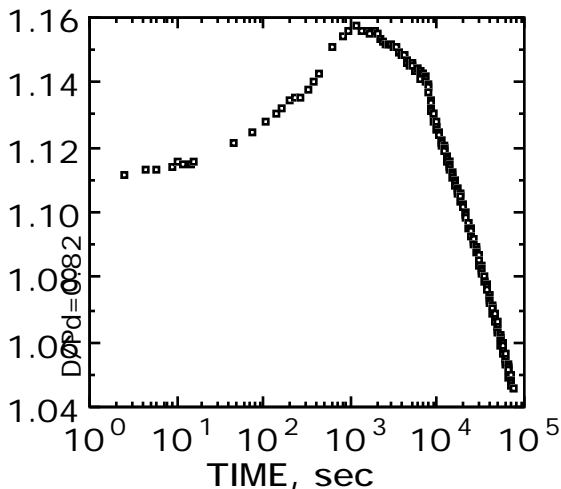


**FIGURE 13.** Deloading of Pd plate #2 in a cell at 40° C

novel crystal-structures in the surface region. Because unknown kinds and amounts of impurity are present in the surface, this behavior can not be correlated with known phases in the pure Pd-D system. However, it does suggest that a hydride, produced using the electrolytic technique, can exhibit unexpected behavior in the surface region.

A few samples having a lower initial deuterium content show a different behavior. Figure 13 describes unannealed palladium as it deloads in the electrolyte. In this case, the OCV initially increases then decreases as deuterium is lost. When plotted as OCV vs D/Pd in Fig. 14, two regions of linear behavior are seen with a transition that does not correspond to any known behavior of the pure Pd-D system. A sample

in general, the higher the OCV, the more complex the behavior. In addition, marked differences in voltage are occasionally found between the two OCV probes, indicating different behaviors between the two sides of the cathode. Samples which were allowed to deload completely generally returned to a zero OCV, showing that surface impurities did not affect the OCV in the absence of deuterium.

## CONCLUSIONS

Results from this and other studies are consistent with the following three conclusions.

1. A fraction of the applied deuterium will recombine to form  $D_2$  before the adsorbed atom can diffuse into the lattice. This fraction is large when the applied current is small especially when a barrier is present on the surface.

2. An atom that dissolves will diffuse toward the nearest interior crack by the normal diffusion, a process which is affected by impurities within the palladium.

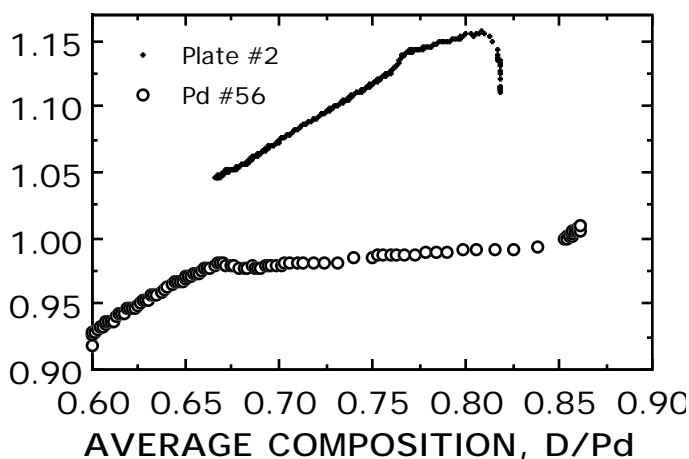


**FIGURE 14.** Change in OCV as a function of average composition during deloading of Pd plate #2 at 40°C and deloading Pd #56 at 21°C is uncorrected for edge-effect.

current is applied frequently reduces the deloading rate. This procedure is proposed to reduce initial stress at the surface. A similar effect may also be produced when high-low current pulses or anodic stripping methods are applied. [34; 35; 36]

**2.** Loading at low current and high temperature appears to reduce the deloading rate. Both conditions are proposed to reduce surface stress.

**3.** Repeated loading and deloading cycles increase the volume of cracks but appear to reduce the effect these cracks have on the deloading rate. This reduction is proposed to be caused by increasing compression in the surface region that closes surface cracks. Impurity deposition into this region may also help by expanding the lattice and collapsing void space.

While gas loss through surface cracks has an influence on the ability to achieve high compositions in the bulk or at spots on the surface, this is not the only important factor. Depending on past treatment, the surface of palladium can acquire a barrier to hydrogen uptake. Although this barrier can be reduced or removed by Aqua Regia or vacuum anneal, electrolytic action can cause a new barrier to form from unavoidable materials within the cell. Such a barrier can result from a layer that blocks ion adsorption or from a reduction in diffusion rate caused by alloy formation between palladium and deposited impurities. On the other hand, formation of certain alloys, Pd-Li alloy for example, may actually help by increasing the diffusion rate through the surface. Aluminum and other metals may make more deuterium ions available by reducing the recombination rate.[37] Surfaces within the cracks, where most of the recombination is proposed to occur, are not in contact with the electrolyte and are, therefore, immune to barrier deposition. Of course, application of a very thick barrier may reduce the loss rate as crack openings are covered over.

Once a limiting composition has been reached, composition gradients are formed with the highest hydrogen content within the surface region. The gradient becomes stable when the rate of H(D) entering the surface equals the rate of gas leaving through the crack structure. Thus, even though the loading efficiency appears to be zero and the composition is stable, a steady flux of deuterium is continuously passing through the surface and diffusing within the metal. This proposed process is in direct conflict with the model that assumes further addition of deuterium is blocked by gas formation at the surface.[38]

**3.** Deuterium gas will leave the structure at a rate proportional to the crack concentration times the effective gas pressure being produced by the hydride at each crack location within the sample. Because the highest composition and pressure exists in the surface region, and because the surface is the source of deuterium, cracks that penetrate the surface are very effective paths for gas loss.

Three procedures have been found to have important effects on the ability to achieve a high deuterium concentration by reducing the effect of cracks.

**1.** Application of small current pulses before the main electrolytic

Low temperature and high current are expected to favor an increase in the average hydrogen concentration both at the surface and in the bulk, as is observed. Because the location of surface cracks is random and any surface barrier will have an uneven thickness, hydrogen concentration at the surface will be very nonuniform. Any effect that is sensitive to composition, such as “cold fusion”, will be influenced by this random, uneven, and difficult to control surface condition.

Changes in the average surface state can be detected using the OCV. When low currents are used, only a small concentration gradient is indicated to exist between the surface and the average bulk composition as long as a mixture of  $\alpha$ - and  $\beta$ -phase is present. Under this condition, the OCV is  $-0.91 \pm 0.02$  V at  $40^\circ$  C referenced to platinum. This is very close to the value reported by Searson [38] who used a Standard-Hydrogen-Electrode in an electrolyte of  $\text{NaOH} + \text{H}_2\text{O}$ . Once the sample has completely converted to  $\beta$ -PdD, the OCV voltage can increase and on rare occasions reach at least  $-1.35$  V. Many variations of this behavior are possible because of unrecognized and uncontrolled changes in surface conditions.

The presence of several new structures on the surface can be inferred from how the OCV changes as deuterium is lost while deloading takes place in the electrolytic cell. Especially interesting is a phase that forms only when the hydrogen activity in the surface is very high and when anomalous heat is apparently produced. [39] These phases are stabilized by surface impurities and some are stable only in a narrow composition range. Their physical and chemical characteristics need to be determined before the “cold fusion” effect can be made predictable or can be properly explained. A study combining X-ray diffraction and OCV measurements would be very useful for this purpose.

Location of surface penetrating fissures can be found by using high resolution SEM[40] or more easily by watching the sample deload while under acetone. Three general features are seen. Bubbles are emitted in isolated spots; they are emitted as intense streams, usually associated with blisters; or they form a line that sometimes can be seen to result from a visible crack or scratch. Most deloading occurs from isolated sites involving one-bubble source suggesting flaws too short to support parallel bubbles. Some samples show large regions from which no bubbles are visible at all. These regions are expected to produce the highest local surface compositions. In contrast, active deloading is observed near the edge because cracks that form perpendicular to the thickness can penetrate the edge to give a high surface density resulting in a reduced concentration. Microscopic examination [41] of the surface of electrolyzing  $\beta$ -PdH has revealed bubbles leaving the surface at the same location whether current is flowing to the cathode, thereby supplying hydrogen atoms to the surface, or whether the sample is being allowed to lose hydrogen in the absence of current. Again, it would appear that much hydrogen gas originates within the hydride structure even when atoms are available for molecule formation or ion exchange at active sites on the surface.

In many cases, the deloading rate in the electrolyte or in acetone is not significantly different from that measured in air. Therefore, reaction with oxygen at the surface does not play an important role in producing deuterium loss. Unfortunately, this is not always the case — as is so typical of palladium. Samples kept in sealed bottles for long periods form liquid water on their surfaces. This water is thought to result from a slow, catalyzed reaction on the palladium surface between already evolved  $\text{D}_2$  and ambient  $\text{O}_2$ . In contrast, a few samples slowly form a little water on their surface during weighing, thereby causing the apparent deuterium loss to be too low. One sample reacted with oxygen so quickly when exposed to air that it became very hot. This very rare event is apparently caused by the deposition of certain impurities on the surface and shows a need for care when palladium hydride is weighed in air, especially in high humidity locations.

A comparison of absolute values between different studies is not possible because several properties are sensitive to the size and geometry of the samples. Because of edge loss, samples having a relatively narrow width will have a greater fraction of their volume affected by this underloaded region. Consequently, such samples will appear to have a smaller than expected average composition. Rods and plates not only have different amounts of edge-loss and end-loss but the crystal morphology differ in both annealed and unannealed material. Sample weight is

also important. For example, the apparent loss rate is sensitive to the mass/area ratio such that less massive samples tend to show a more rapid change in D/Pd than do heavier samples. For these reasons, only trends in behavior have a useful meaning.

## ACKNOWLEDGMENT

This work would not have been possible without the financial help provided by Dr. Dave Nagel (NRL) and Fred Jaeger (ENECO). The author is also grateful to Mr. Yoshihisa Kamiya and Mr. Toshihisa Terazawa of the IMRA Materials Laboratory, and Dr. Keiji Kunimatsu of IMRA Japan for providing the samples.

## REFERENCES

- [1] All properties discussed in this paper apply equally to the palladium hydride as well as the palladium deuteride.
- [2] A. M. Riley, J. D. Seader, and D. W. Pershing, *J. Electrochem. Soc.* **139**, 1342 (1992).
- [3] A. De Ninno, A. La Barbera and V. Violante, Progress in Hydrogen Energy (M. Okamoto, ed.), Proc. 6th International Conference on Cold Fusion, Hokkaido, Japan, Oct. 13-18, 1996, Vol. 1, page 192.
- [4] T. B. Flanagan and W. A. Oates, *Annu. Rev. Mater. Sci.* **21**, 269 (1991).
- [5] R. C. Salvarezza, M. C. Montemayor, E. Fatas and A. J. Arvia, *J. Electroanal. Chem.* **313**, 291 (1991).
- [6] B. E. Conway and J. Wojtowicz, *J. Electroanal. Chem.* **326**, 277 (1992).
- [7] S. Szpak, P. A. Mosier-Boss and C. J. Gabriel, *J. Electroanal. Chem.* **365**, 275 (1994).
- [8] C. -C. Hu and T.-C. Wen, *J. Electrochem. Soc.* **142**, 1376 (1995).
- [9] T. B. Flanagan and W. A. Oates, *Ann. Rev. Mater. Sci.* **21**, 269 (1991).
- [10] R. A. Oriani, *Trans. Fusion Technol.* **26**, #4T (1994) 235.
- [11] B. G. Pound, in J. O'M. Bockris, B. E. Conway and R. E. White (eds.), *Modern Aspects of Electrochemistry*, vol. 25, Plenum, New York, 1993.
- [12] J. O'M. Bockris and P. K. Subramanyan, *Electrochim. Acta* **16**, 2169 (1971).
- [13] D.P. Smith and G. J. Derge, *Trans. Electrochem. Soc.* LXVI, 253 (1935).
- [14] F. De Marco, A. De Ninno, A. Frattolillo, A. La Barbera F. Scaramuzzi, and V. Violante, Progress in Hydrogen Energy (M. Okamoto, ed.), Proc. 6th International Conference on Cold Fusion, Hokkaido, Japan, Oct. 13-18, 1996, Vol. 1, page 145
- [15] E. Storms. and C. Talcott-Storms, *Fusion Technol.* **20**, 246 (1991).
- [16] F. A. Lewis, "The Palladium Hydrogen System", Academic Press, N. Y. 1967.
- [17] Z. S. Minevski, Ph. D. Thesis, Texas A & M University, Collage Station, TX, (1995).
- [18] N. Oyama, M. Ozaki, S. Tsukiyama, O. Hatozaki and K. Kunimatsu, Progress in Hydrogen Energy (M. Okamoto, ed.), Proc. 6th International Conference on Cold Fusion, Hokkaido, Japan, Oct. 13-18, 1996, Vol. 1, page 234.
- [19] O. Yamazaki, H. Yoshitake, N. Kamiya, and K. Ota, *J. Electroanal. Chem.* **390**, 127 (1995).
- [20] F. Dalard, M. Ulmann, J. Augustynski, and P. Selvam, *J. Electroanal. Chem.* **270**, 445 (1989).
- [21] C. J. Lihn, C. C. Wan, C. M. Wan, and T. P. Perng, *Fusion Technology* **24**, 324 (1993).
- [22] F. Dalard, M. Ulmann, J. Augustynski, and P. Selvam, *J. Electroanal. Chem.* **270**, 445 (1989).
- [23] M. Ulmann, J. Liu, J. Augustynski, F. Medi, and L. Schlapbach, *J. Electroanal. Chem.* **286**, 257 (1990).
- [24] E. Storms, *Infinite Energy* **1**, #5 & 6, 77 (1996).
- [25] F. L. Tanzella, S. Crouch-Baker, A. McKeown, M. C. H. McKubre, M. Williams and S. Wing, Progress in Hydrogen Energy (M. Okamoto, ed.), Proc. 6th International Conference on Cold Fusion, Hokkaido, Japan, Oct. 13-18, 1996, Vol. 1, page 171.

- [26] H. Numata and I. Ohno, Progress in Hydrogen Energy (M. Okamoto, ed.), Proc. 6th International Conference on Cold Fusion, Hokkaido, Japan, Oct. 13-18, 1996, Vol. 1, page 213.
- [27] T. Terazawa, T. Sano, Y. Kamiya, Y. Oyabe and T. Ohi, Progress in Hydrogen Energy (M. Okamoto, ed.), Proc. 6th International Conference on Cold Fusion, Hokkaido, Japan, Oct. 13-18, 1996, Vol. 1, page 179.
- [28] National Instruments, Austin, TX
- [29] A. De Ninno, A. La Barbera and V. Violante, Progress in Hydrogen Energy (M. Okamoto, ed.), Proc. 6th International Conference on Cold Fusion, Hokkaido, Japan, Oct. 13-18, 1996, Vol. 1, page 192.
- [30] M. C. H. McKubre, S. Crouch-Baker, A. K. Hauser, S. I. Smedley, F. L. Tanzella, M. S. Williams, S. S. Wing, Proc. Fifth International Conference on Cold Fusion, 9-13 April 1995, Monte Carlo, Monaco, p. 17.
- [31] E. Storms. and C. Talcott-Storms, *Fusion Technol.* **20**, 246 (1991).
- [32] P. C. Searson, *Acta metall. mater.* **39**, 2519 (1991).
- [33] T. Green and D. Britz, *J. Electroanal. Chem.* **412**, 59 (1996).
- [34] A. De Ninno, A. La Barbera and V. Violante, Progress in Hydrogen Energy (M. Okamoto, ed.), Proc. 6th International Conference on Cold Fusion, Hokkaido, Japan, Oct. 13-18, 1996, Vol. 1, page 192.
- [35] E. Ragland, *Infinite Energy* **2**, #10, 22 (1996). Also presented at the Sixth International Conference on Cold Fusion, Oct. 13-18, 1996, Toya, Japan.
- [36] A. Takahashi, Proc. Int. Symp. Nonlinear Phenom. in Electromagnetic Fields, ISEM-Nagoya, Japan, Jan. 27-29, 1992.
- [37] M. C. H. McKubre, S. Crouch-Baker, A. K. Hauser, S. I. Smedley, F. L. Tanzella, M. S. Williams, S. S. Wing, Proc. Fifth International Conference on Cold Fusion, 9-13 April 1995, Monte Carlo, Monaco, p. 17.
- [38] P. C. Searson, *Acta metall. mater.* **39**, 2519 (1991).
- [39] E. Storms, *Infinite Energy* **2**, #8, 50 (1996).
- [40] H. K. An, E. J. Jeong, J. H. Hong and Y. Lee, *Fusion Technol.* **27**, 408 (1995).
- [41] H. Randolph, Westinghouse Savannah River Laboratory, Private Communication (1989).

**TABLE 1**  
Summary of Excess Volume (EV), Limiting Composition (D/Pd),  
Deloading Rate (DL), and Open-Circuit-Voltage (OCV)

#	PRETREATMENT	D/Pd	DL*	- OCV	LOADING METHOD
5(7)	A1-B1, PL	0.82	11.0	1.08	μL, 50 mA, 40°C
11	A1-B1, AR	0.85	8.2	1.09	μL, 50 mA, 40°
36	A1-B2	0.80	0.9	1.07	μL, 50 mA, 40°
43	A1-B4, PL, AR	0.69	5.1	1.00	μL, 50 mA, 40°
21	A1-B1	0.86	6.5	1.13	μL, 800 mA, 40°
22	A1-B1	0.85	8.4	1.04	μL, 800 mA, 7°
8	A1-B1	0.79	5.0	0.90	980 mA, 50°
10	A1-B1	0.85	15.0	0.90	800 mA, 27°
13	A1-B1	0.86	14.4	0.90	800 mA, 27°
14	A1-B1	0.84	13.1	0.92	800 mA, 32°
16	A1-B1	0.82	21.9	1.01	800 mA, 45°
20	A1-B1	0.87	16.9	0.93	800 mA, 28°
60	A2-B1	0.83	15.2	0.93	800 mA, 33°
56	A2-B1	0.88	8.2		100 mA, 6°
57	A2-B1	0.88	14.3		100 mA, 6°
58	A2-B1	0.85	10.4		100 mA, 5°
82	A2-B2	0.79	14.1		100 mA, 6°
7	A1-B1	0.79	8.4	0.84	100mA, 20°
15	A1-B1	0.73	4.0	0.68	49 mA, 31°
19	A1-B1	0.81	13.5	0.83	100 mA, 20°
23	A1-B1	0.86	8.2	0.87	100 mA, 21°
26	A1-B1	0.82	9.4	0.83	100 mA, 21°
52	A2-B1	0.82	12.5	0.81	100 mA, 20°
54	A2-B1	0.83	11.0	0.84	100 mA, 20°
61	A2-B1	0.80	7.8	0.87	100 ma, 20°
78	A2-B1	0.79	9.9	0.83	100 mA, 21°
79	A2-B1	0.86	7.4	0.83	100 mA, 20°

\* D/Pd/ min x1000

A1 = Pure palladium

A2 = 500 ppm Boron Added

B1 = Basic treatment (Arc melt, cast, swag, roll, cut, polish with 0.5 μm diamond)

B2 = Basic + annealed in air at 750°C for 24 hr.

B3 = Basic + anneal in poor vacuum at 750°C for 24 hr

B4 = Basic + B3 + AR

AR =Etched in Aqua Regia

μL = Preloaded using pulsed current.

PL = Previously loaded and deloaded

**TABLE 2**  
Effect of cycled loading on properties of Pd #5 and #21

#	Treatment	Fraction of Initial Value			Deloading Rate*	-OCV	D/Pd
		Width	Length	Thickness			
<b>#5 (A1-B1)</b>							
1	Loaded	1.02	1.01	1.12			0.80
2	Deloaded	0.98	0.98	1.07			0.00
3	Loaded	1.01	1.01	1.15			0.82
4	Deloaded	0.97	0.98	1.10			0.00
5	Loaded	1.01	1.00	1.18	<1	1.08	0.82
6	Deloaded**	0.97	0.97	1.09			0.00
7	Loaded	0.99	0.99	1.23	11.6	1.07	0.85
8	Deloaded**	0.95	0.95	1.15			0.00
9	Loaded	0.98	0.96	1.29	2.2	1.04	0.80
10	Deloaded**	0.95	0.94	1.21			0.00
11	Loaded	0.97	0.96	1.34	2.8	1.08	0.82
12	Deloaded**	0.94	0.92	1.26			0.00
13	Loaded	0.97	0.94	1.40	2.0	1.04	0.81
14	Deloaded**	0.93	0.91	1.29			0.00
15	Loaded	0.97	0.93	1.45	1.2	1.10	0.82
16	Deloaded**	0.93	0.90	1.36			0.00
Etched using Aqua Regia							
17	Loaded				2.9	1.07	0.79
<b>#21(A1-B1)</b>							
1	Loaded	1.028	1.019	1.116		1.12	0.85
2	Deloaded	0.986	0.984	1.063			0.00
3	Loaded	1.012	1.004	1.179		1.13	0.83
4	Deloading***	1.008	1.000	1.176			0.75
5	Loaded	1.015	1.005	1.186		1.10	0.85
<b>#36 (A1-B3)</b>							
1	Loaded	1.022	1.027	1.108	0.9	1.07	0.80
2	Deloaded	0.990	0.990	1.032			0.00
3	Loaded	1.007	1.017	1.140	4.3	1.11	0.84
4	Deloaded	0.972	0.979	1.071			0.00
5	Loaded	0.991	1.005	1.194	2.0	1.15	0.84
6	Deloaded	0.970	0.957	1.120			0.00
7	Loaded	1.004	0.979	1.210	1.6	1.09	0.82

\* D/Pd/ min x1000  
 \*\* Deloaded at 170°C  
 \*\*\* Partial deloading  
 all dimension in cm